

Unusual Thixotropic Properties of Aqueous Dispersions of Laponite RD

NORBERT WILLENBACHER¹

BASF AG, Polymer Research Division, 67056 Ludwigshafen, Germany

Received November 10, 1995; accepted April 17, 1996

The rheological properties of aqueous dispersions of the synthetic hectorite clay Laponite RD that form gel-like structures have been investigated. Special emphasis has been laid on the phenomenon of thixotropy. Structural recovery at rest after steady shear is considered a fundamental thixotropic process and has been characterized by small amplitude oscillatory shear measurements. A special sealing technique was used to prevent the evaporation of water during these experiments. After cessation of steady shear $|\eta^*|$ increases monotonically with time and even after 16 days no equilibrium viscosity value is reached. A single power law $|\eta^*| \sim t^n$ holds within the time regime from 10 to 10^6 s. The exponent $n = 0.13 \pm 0.02$ is independent of clay concentration and mechanical pre-treatment of the material. This type of kinetics has not been reported so far for the thixotropic recovery of any clay dispersion and it does not fit the common definition of thixotropy. The reorganization of the gel structure determining this thixotropic phenomenon is interpreted as a cooperative self delaying process similar to the aging of glassy polymers or precipitation from supersaturated solid solutions. © 1996 Academic Press, Inc.

Key Words: clay; flocculated dispersion; thixotropy.

INTRODUCTION

Clay minerals of the montmorillonite or hectorite type are able to form three-dimensional gel-like structures when dispersed in aqueous media. Therefore, these materials are commonly used as thickening, plasticizing, or emulsifying agents in various industrial products such as paints, plasters, adhesives or cosmetical formulations. Consequently extensive studies have been reported on their colloidal and rheological properties (Refs. 1–4).

Laponite RD (Laporte Inc., UK) is a fully synthetic clay similar in structure and composition to natural hectorite of the smectic group. Each layer comprises three sheets, two outer tetrahedral silica sheets and a central octahedral magnesium sheet. Part of the magnesium in the central sheet is replaced by lithium, resulting in a net negative charge of the layer, which is balanced by sodium ions located between adjacent layers in a stack. The idealized chemical formula is $[(\text{Si}_8(\text{Mg}_{5.34}\text{Li}_{0.66})\text{O}_{20}(\text{OH})_4)\text{Na}_{0.66}]$. The sodium ions are

exchangeable and in aqueous dispersions these ions diffuse into the water and plate-like particles with negatively charged faces are formed. The charge on the oxide edge of the platelets is less negative or even positive depending upon the pH of the dispersing medium. The average size of these particles is 30 nm in diameter and 1–4 nm in height, as revealed by electron microscopy (5, 6) and independently confirmed by various scattering techniques (6–8) and ultracentrifuge analysis (8). Thus these particles are an order of magnitude smaller than those in refined natural clays.

Generally, two different mechanisms for gelation in clay mineral dispersions are proposed, leading to different types of three-dimensional ordering. In the first case the formation of an equilibrium structure is induced by long-range electrostatic repulsion between interacting double-layers. This mechanism, which has been proposed by Norrish (9) and supported by experiments of Callaghan and Ottewill (10), accounts for gel formation at low electrolyte concentration ($<10^{-3}$ mol dm^{-3} , 1:1 electrolyte). At higher ionic strength another mechanism suggested by van Olphen (1, 11) is favored: the double layers around the faces of the platelets are compressed and the electrostatic attraction between oppositely charged faces and edges, together with the attractive van der Waals forces between the particles, gives rise to edge-to-face as well as edge-to-edge associations, leading to a linked, three-dimensional network (house of cards).

Nevertheless, particle interaction and structure formation in gelled clay dispersions are still a matter of debate.

Due to its high purity and narrow particle size distribution Laponite has served as a model clay system and has been investigated under various conditions of electrolyte content, pH range, and clay concentration. Static and dynamic light scattering data support the formation of tactoids consisting of several platelets (7). A spatially heterogeneous structure of isolated particles with local orientational correlation has been suggested on the basis of small angle X-ray and neutron scattering experiments (12, 13) and has been evidenced by cryofracture electron microscopy (14). In addition, correlations between macroscopic electrical (15) and rheological properties (16) and microstructure have been attempted.

Furthermore, a phase diagram has been established (14) and fundamental colloidal and surface properties of swelling

¹ E-mail: norbert.willenbacher@zkm.x400.basf-ag.de.

clays, such as stability of sols in the presence of electrolytes (17), surface charge characteristics and cation exchange capacity (6), and the adsorption of water on the clay particles (18) have been studied. The kinetics of gelation of aqueous Laponite dispersions has been rheologically probed by transient measurements of the storage modulus G' (16).

Due to its application as an emulsifying and thickening agent, the rheology of dispersions of Laponite is of particular technical interest. Hence the stabilizing and thickening efficiency of Laponite in pigment suspensions and polymer dispersions (5), as well as the gelation and flocculation of dispersions of Laponite caused by addition of electrolytes or polar solvents, has been evaluated by rheological measurements (19). Furthermore, rheological properties of blends of Laponite and polymeric thickeners (such as carboxymethylcellulose, xanthan gum, or polyacrylic acid) have been studied (20).

This paper concentrates on an accurate experimental determination of the rheological properties of flocculated dispersions of Laponite RD, such as viscoelasticity, yield stress, and thixotropy. Special emphasis is laid on the phenomenon of thixotropy, which is typical not only for Laponite but also for natural clay gels. The recovery of the equilibrium rest state after steady shear is considered a fundamental thixotropic process. Small amplitude oscillatory shear measurements are used to determine the kinetics of this process. Various conditions of preshearing and gels of various concentrations are examined. This approach to the characterization of dynamic processes in thixotropic materials was originally introduced by Mewis and de Bleyser and its feasibility was demonstrated using a polyamide gel as a model system (21). Moreover, the method is commonly used to study the gelation kinetics of clay dispersions (4, 16, 22).

EXPERIMENTAL

Materials

Laponite RD is a commercial material from Laporte Inc., UK, and was used without further purification. Aqueous dispersions of Laponite with concentrations between 1% and 3% w/w were prepared using NaCl solutions of various ionic strengths between 0.0017 and 0.052 mol/dm³ as dispersing agents. The required amount of the crystalline powder is added to the solution of the desired salinity and the dispersion is rapidly stirred for about 15 min. Gelation takes place within a period from a few hours up to some days depending on concentration of clay and electrolyte, respectively. Therefore, samples were allowed to age for at least 1 week at room temperature before rheological measurements were started. The pH of the samples was 9.6.

Measurements

Oscillatory shear experiments were performed on a controlled strain rate instrument (RFS 8400, Rheometrics Inc.,

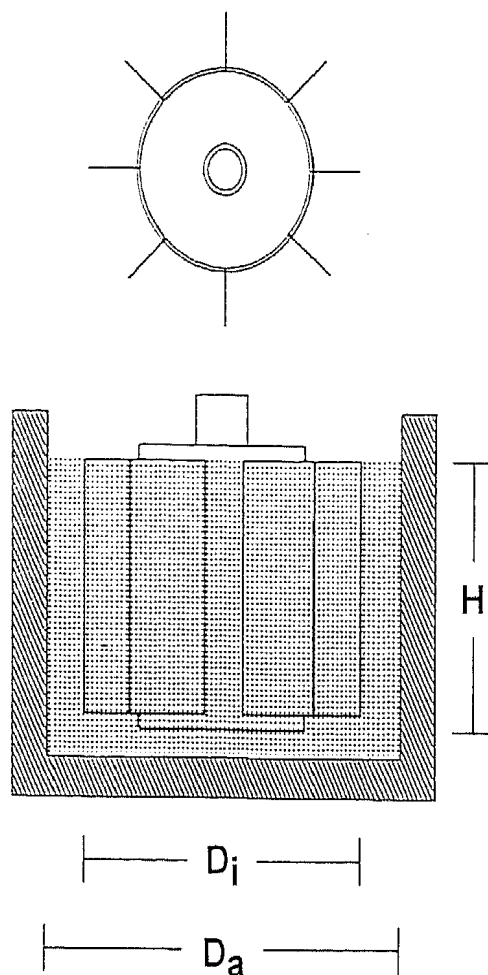


FIG. 1. Schematic representation of the vane geometry (top and side views).

USA) using cone/plate- and plate/plate-geometry. In this experiments the sample is exposed to a sinusoidal strain $\gamma = \hat{\gamma} \sin \omega \cdot t$ and the stress response τ is recorded. In the linear viscoelastic regime the storage modulus G' and the loss modulus G'' are determined from an harmonic analysis of the stress signal. The absolute value of the complex viscosity $\eta^* = (1/\omega)(G'' - iG')$ is given by $|\eta^*| = \omega^{-1} \sqrt{G'^2 + G''^2}$.

Evaporation of water during long-term (up to 16 days) oscillatory shear experiments was prevented by covering the samples with a 5 mm layer of vacuum pump oil (Pfeiffer GmbH, Germany) with $\eta = 196 \text{ mPa} \cdot \text{s}$ at $T = 25^\circ\text{C}$. Note that the sealing liquid has to be chosen carefully. Whereas the water loss is about 3% within a period of 16 days when the vacuum pump oil is used, more than 30% of the water evaporated within the same time when the sample was covered by a silicon oil with $\eta = 970 \text{ mPa} \cdot \text{s}$ at $T = 25^\circ\text{C}$ (Baysilone M 1000, Bayer AG, Germany).

Creep and creep recovery experiments were carried out using a controlled stress instrument (CS 100, Carri-Med Ltd., UK) equipped with a vane geometry (23) as shown in Fig. 1 in order to avoid wall slip effects. The dimensions of the vane

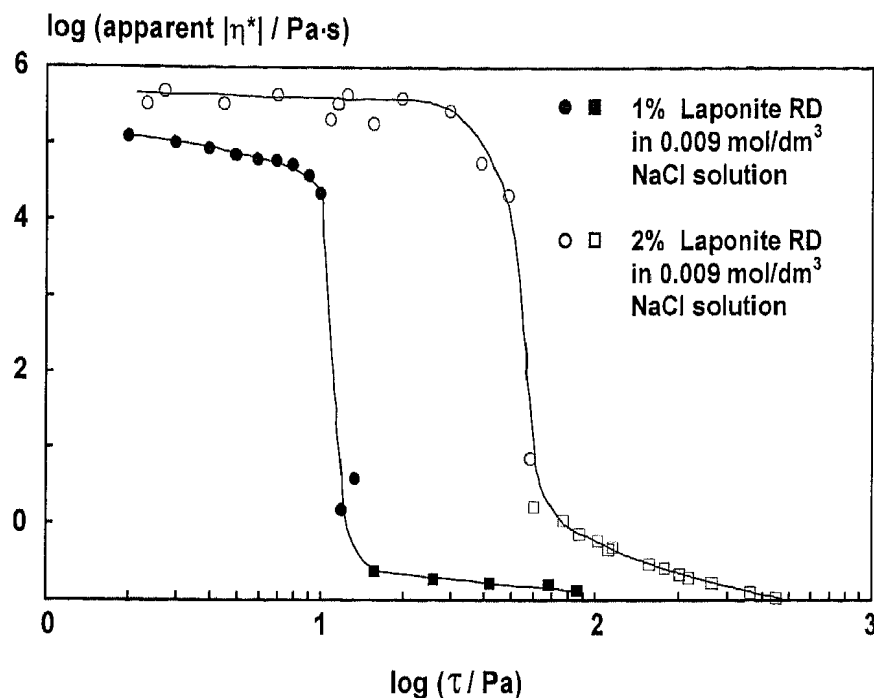


FIG. 2. Apparent viscosity vs shear stress as obtained by creep tests (○, ●) and capillary viscometry (□, ■) for 1% and 2% w/w dispersions of Laponite RD in 0.009 mol/l NaCl solution.

are $H = 26.5$ mm, $D_i = 28$ mm, and $D_a = 48$ mm. The shear stress is calculated from the applied torque T by

$$\tau = 2T/\pi D_i^3 \left(\frac{H}{D_i} + \frac{1}{6} \right). \quad [1]$$

Steady shear viscosity data were obtained with a home-made piston-driven capillary viscometer (KVM). Dies of different length over radius ratios L/R were used to estimate entrance pressure loss and wall slip effects.

RESULTS AND DISCUSSION

Apparent Yield Stress

The viscosities of a 1% w/w and a 2% w/w dispersion of Laponite RD in 0.009 mol/dm³ NaCl-solution as a function of shear stress are shown in Fig. 2. In both cases a critical shear stress τ_c is observed at which the viscosity changes by more than six orders of magnitude. The viscosity data at shear stresses $\tau \leq \tau_c$ were calculated from creep tests carried out using a vane geometry. The samples were not deformed homogeneously throughout the whole rheometer gap in these experiments. As can be seen from Fig. 3a, the deformation was restricted to a narrow circular path of approximately 1–2 mm in width directly at the vane where the torque was acting. Therefore, the viscosity data which were calculated from the measured angular displacement assuming a deformation of the sample throughout the gap are not correct and must be regarded as apparent viscosity values. From the ratio of the de-

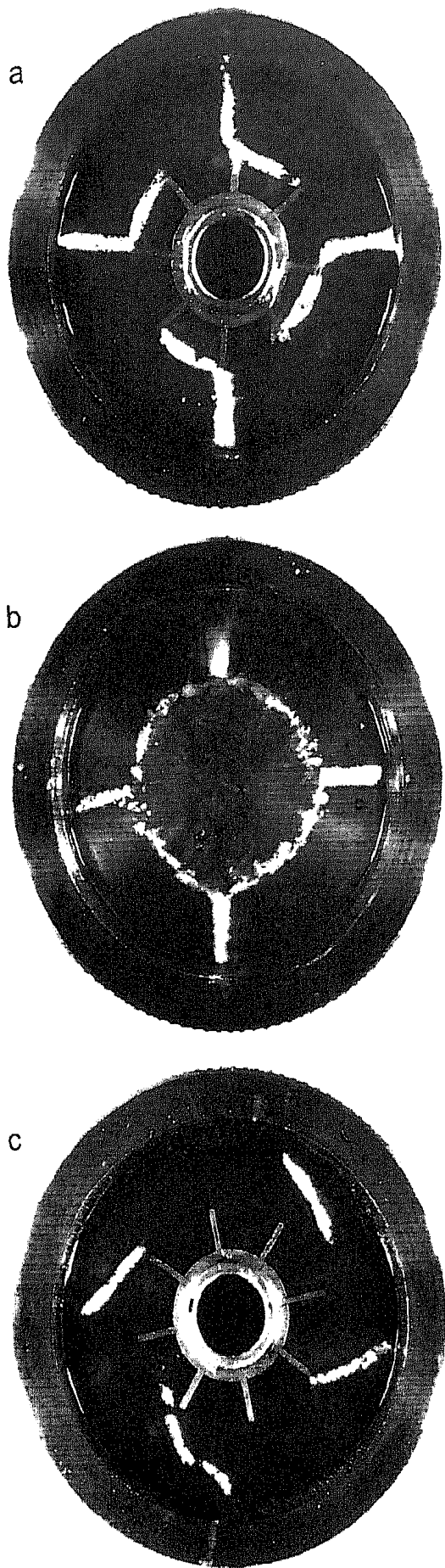
formed layer thickness to the total gap width the true values are estimated to be about one order of magnitude lower.

Furthermore, these data are not equilibrium values. Due to the unusual thixotropic nature of this material (see below), even in creep experiments lasting for several days no true steady state is reached. The creep tests considered here lasted 15 min and the samples were kept at rest for 20 min before the measurements started in order to reduce the influence of the mechanical treatment associated with the deposition of the sample into the rheometer. A fresh sample was used for each measurement. The creep experiments were restricted to the shear stress range below τ_c , since the upper limit of the angular velocity of the controlled stress rotational rheometer was reached when τ_c was exceeded.

The data at shear stresses above τ_c , marked by squares in Fig. 2, were obtained using a controlled shear rate capillary viscometer equipped with a die of 400 mm in length and 0.6 mm in radius. Preceding experiments did show that entrance pressure losses and wall slip effects could be neglected in this case. Shear stress data were calculated from apparent viscosity and shear rate values as $\tau = \eta \cdot \dot{\gamma}$.

Viscoelasticity

The dynamic moduli G' and G'' of aqueous dispersions of Laponite RD have been determined by oscillatory shear experiments. Typical results for the dependence of G' and G'' on strain amplitude and angular frequency are shown in Figs. 4a and b, respectively, for a 1% w/w dispersion of Laponite RD in 0.009 mol/dm³ NaCl solution. Similar re-



sults were obtained for dispersions of different ionic strength and clay concentration, respectively.

For strain amplitudes < 0.01 linear viscoelastic behavior is observed and G' is more than one order of magnitude larger than G'' . Moreover, G' stays constant up to a critical strain amplitude $\hat{\gamma}_c$ (≈ 0.15), but decreases drastically when $\hat{\gamma} > \hat{\gamma}_c$. On the other hand G'' goes through a maximum at $\hat{\gamma}_c$ and dominates over G' at strain amplitudes $\hat{\gamma} > 0.5$. The dependence of G' and G'' on angular frequency in the linear viscoelastic regime is shown in Fig. 4b. The storage modulus G' dominates over G'' by more than one order of magnitude and is essentially independent of ω in the whole frequency range investigated (10^{-3} – 10^2 s^{-1}). As a consequence $|\eta^*|$ varies proportional to ω^{-1} .

The viscoelastic features reported in this section are typical for materials with a three-dimensional gel-like structure and the results are in good agreement with those reported previously by Mourchid *et al.* (14) for Laponite dispersions of nearly the same ionic strength. Similar results are reported for dispersions of low ionic strength (10^{-3} mol/dm³ NaCl) (16).

Thixotropy

The re-creation of the equilibrium rest structure after shearing is considered as a fundamental thixotropic process. This process has been investigated by transient oscillatory shear experiments and for convenience the kinetics of the thixotropic recovery is characterized by the time dependence of $|\eta^*|$. Alternatively, the time dependence of G' could have been discussed, as for example in (4, 21, 22). For the systems investigated here, this is completely equivalent, since $G' \gg G''$ even for the first data points taken about 10 s after cessation of steady shear. For convenience the oscillation frequency was set to $\omega = 6.28$ s^{-1} for all experiments discussed in the following chapter, as long as nothing else is mentioned.

The oscillation experiments had to be carried out at sufficiently small strain amplitudes in order to avoid a disturbance of the recovery process.

In Fig. 5 the development of $|\eta^*|$ after cessation of steady shear (30 s at $\dot{\gamma} = 1000$ s^{-1}) is shown for different amplitudes of oscillation $\hat{\gamma}$ between 0.01 and 1 applied to a 1% w/w dispersion of Laponite RD in 0.009 mol/dm³ NaCl-solution. In all cases a sharp increase of $|\eta^*|$ is observed within the first few seconds after cessation of steady shear. At high strain amplitudes ($\hat{\gamma} = 0.8$ and 1), where viscous properties prevail, a steady state viscosity is approached im-

FIG. 3. Sample deformation during creep tests using the vane geometry visualized through the deformation of four lines of white chalk powder spread on top of the sample before running the measurement: (a) 3% w/w Laponite RD in deionized water, creep test at $\tau < \tau_c$; (b) 3% w/w Laponite RD in deionized water, creep test at $\tau > \tau_c$ (picture taken after several revolutions of the vane); (c) for comparison, silicon oil Baysilone M 1000 (homogeneous deformation throughout the gap).

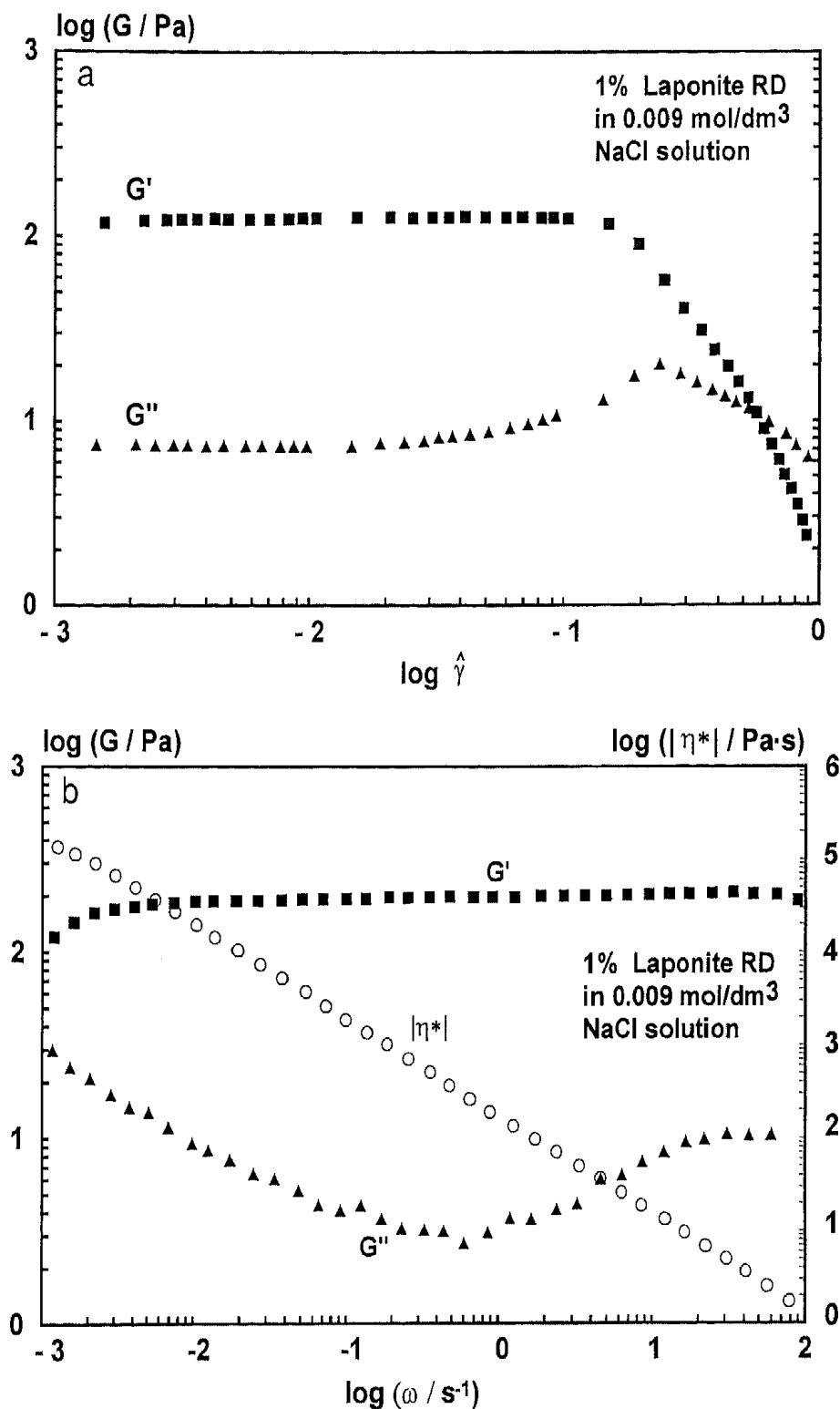


FIG. 4. (a) Dynamic moduli G' and G'' vs strain amplitude $\hat{\gamma}$ and (b) dynamic moduli G' , G'' , and complex viscosity $|\eta^*|$ vs angular frequency ω for a 1% w/w dispersion of Laponite RD in 0.009 mol/l NaCl-solution (sample was allowed to equilibrate for 15 min before the measurement was started).

mediately after this first increase, whereas $|\eta^*|$ goes through a maximum about 50 s after cessation of steady shear and reaches an equilibrium value (depending on $\hat{\gamma}$) after about 500 s, when intermediate oscillation amplitudes ($\hat{\gamma} = 0.4$ and 0.5) are applied. In contrast, the absolute value of the complex viscosity grows monotonically and independent of the chosen strain amplitude, as long as $\hat{\gamma} \leq \hat{\gamma}_c$.

Similar experiments have been performed on a 2% w/w dispersion of Laponite RD in 0.009 mol/dm³ NaCl-solution. The results obtained for $\hat{\gamma} \leq \hat{\gamma}_c$ are shown in Fig. 6. $\log |\eta^*|$ increases in proportion to $\log t$ and no equilibrium viscosity value is reached, even after more than 16 h.

This is the key result of the present investigation and further experiments have been performed to prove that this

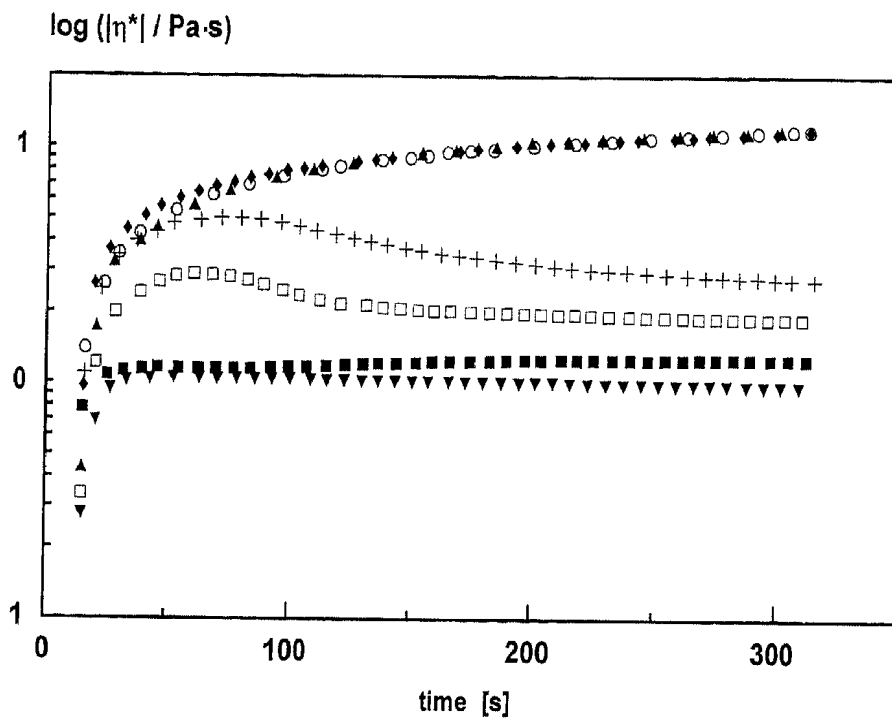


FIG. 5. Effect of oscillation amplitude $\dot{\gamma}$ on the recovery of $|\eta^*|$ after cessation of steady shear ($t = 30$ s; $\dot{\gamma} = 1000$ s $^{-1}$) for a 1% w/w dispersion of Laponite RD in 0.009 mol/l NaCl-solution for $\dot{\gamma} = 0.01$ (◆), 0.05 (○), 0.2 (▲), 0.4 (+), 0.5 (□), 0.8 (■), 1.0 (▼) at oscillation $\omega = 6.28$ s $^{-1}$.

unusual result really reflects a material property and not an experimental artefact.

The results of oscillatory shear experiments presented above were obtained in a computer-controlled, automatic operation procedure. In this experimental mode the sample is exposed to a permanent oscillatory shearing. A comparison of the transient viscosity data obtained by this procedure

to results gained from manually controlled experiments is shown in Fig. 7. In the latter case the fluid is sheared only for a few periods of oscillation, when a data point is registered and the sample is kept at rest in the meantime. Obviously it does not make any difference whether the material is under continuous small amplitude oscillatory shear or not. Therefore it is concluded, that the observed increase in vis-

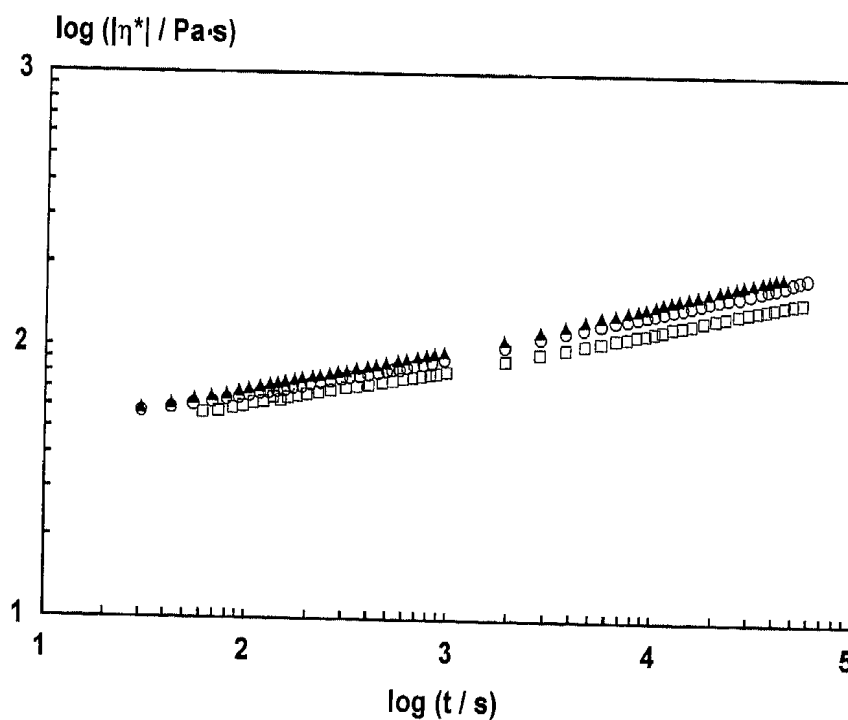


FIG. 6. Recovery of $|\eta^*|$ after cessation of steady shear ($t = 30$ s; $\dot{\gamma} = 1000$ s $^{-1}$) for various oscillation amplitudes $\dot{\gamma} < \dot{\gamma}_c$ for a 2% w/w dispersion of Laponite RD in 0.009 mol/dm 3 NaCl-solution with $\dot{\gamma} = 0.07$ (▲), 0.05 (○), 0.01 (□) at oscillation $\omega = 6.28$ s $^{-1}$.

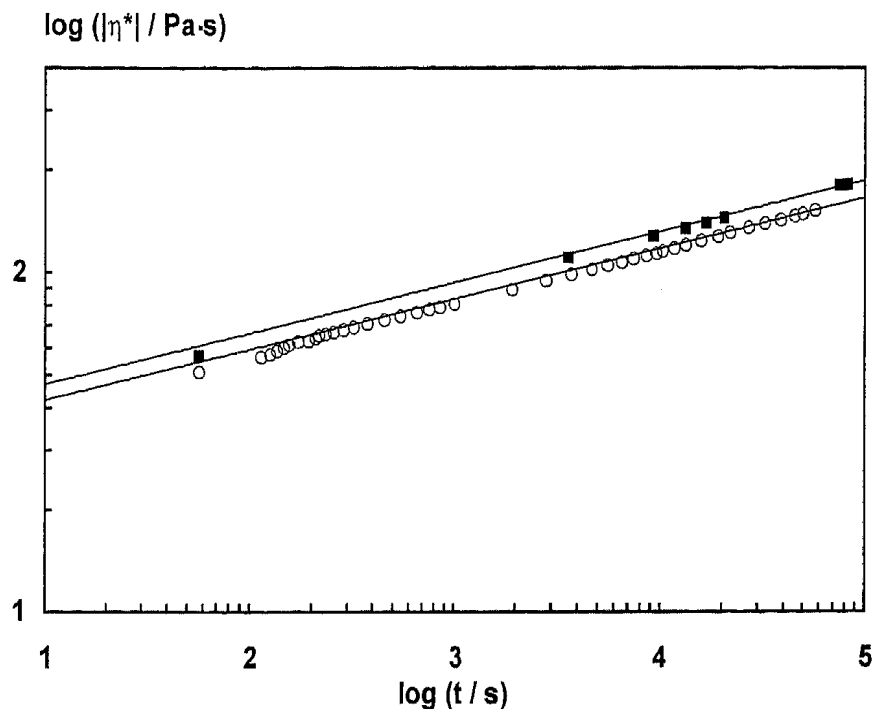


FIG. 7. Effect of oscillation mode on the recovery of $|\eta^*|$ after cessation of steady shear ($t = 30$ s; $\dot{\gamma} = 1000$ s $^{-1}$) for a 2% w/w dispersion of Laponite RD in 0.009 mol/dm 3 NaCl-solution: (■) oscillation only during acquisition of data points, (○) permanent oscillation, where $\omega = 6.28$ s $^{-1}$, $\dot{\gamma} = 0.01$.

cosity is not a rheopexy or work-hardening phenomenon (1). The small offset between the two data sets is presumably due to differences in the pretreatment of the respective sample.

The influence of different mechanical pretreatment and preshearing procedures on the recovery of $|\eta^*|$ is shown in Fig. 8 for a 1% w/w dispersion of Laponite RD in 0.009

mol/dm 3 NaCl-solution. The slope of the log $|\eta^*|$ vs log t curves is virtually independent of the sample history. But the viscosity level decreases as the total amount of mechanical energy brought into the material is increased.

The recovery of $|\eta^*|$ after cessation of steady shear has been studied for various clay concentrations between 1%

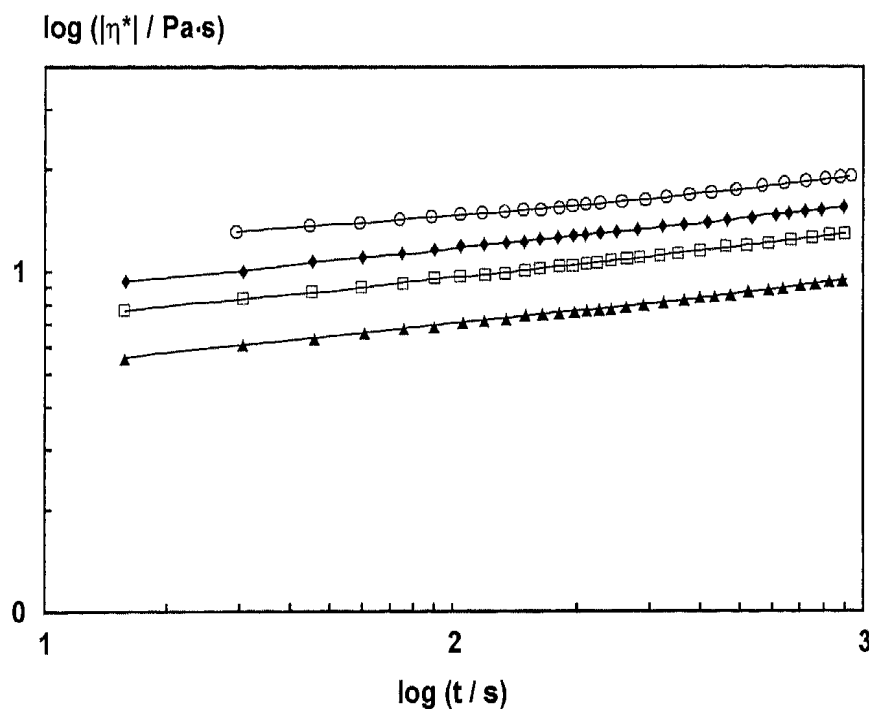


FIG. 8. Effect of sample history/mechanical pretreatment on the recovery of $|\eta^*|$ for a 1% w/w dispersion of Laponite RD in 0.009 mol/dm 3 NaCl-solution: (○) careful placement of sample in rheometer, (◆) intensive stirring before placement in rheometer, (□) careful handling + preshearing ($\dot{\gamma} = 1000$ s $^{-1}$, $t = 600$ s), (▲) intensive stirring + preshearing, where oscillation $\omega = 6.28$ s $^{-1}$, $\dot{\gamma} = 0.01$.

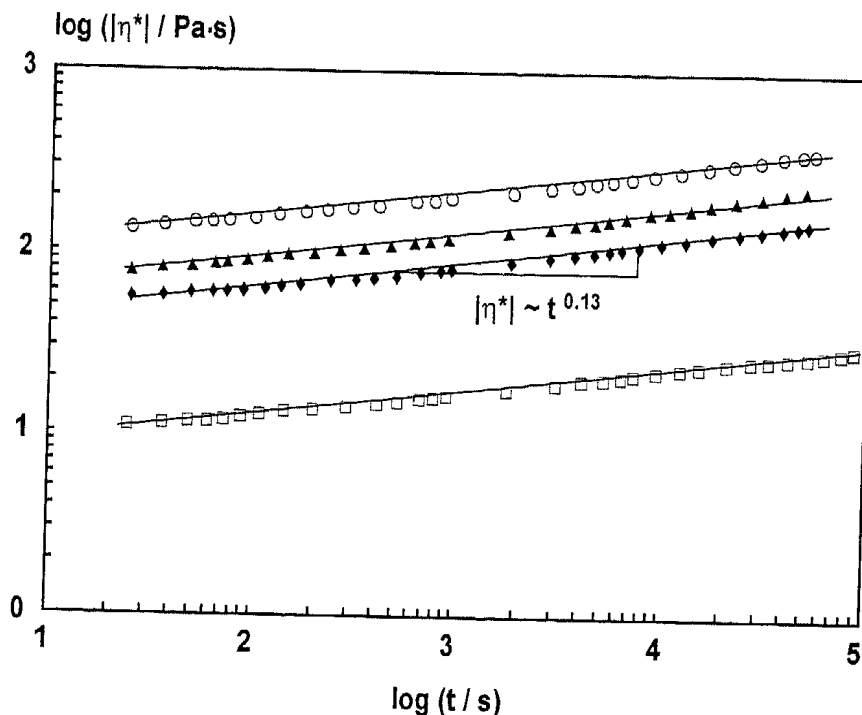


FIG. 9. Recovery of $|\eta^*|$ after cessation of steady shear ($t = 30$ s; $\dot{\gamma} = 1000$ s $^{-1}$) for dispersions of various concentration of Laponite RD in 0.009 mol/dm 3 NaCl-solution: concentration 3% (O), 2.5% (\blacktriangle), 2% (\blacklozenge), 1% (\square), with oscillation $\omega = 6.28$ s $^{-1}$, $\hat{\gamma} = 0.01$.

and 3% w/w (Fig. 9). The mechanical pretreatment was the same for each sample. In all cases a linear increase of $\log |\eta^*|$ with $\log t$ is observed and no equilibrium viscosity value was reached. Moreover, the slope of the straight lines fitted to the experimental data points is the same for all clay concentrations.

The experiments presented so far were limited to a period of 16 h after cessation of steady shear. One experiment was carried out lasting for 16 days (1.4×10^6 s $^{-1}$). But even on this extended time scale no equilibrium viscosity value $|\eta^*|$ was reached (Fig. 10). Especially in such long term measurements one has to take care that the evaporation of water is prevented. Therefore this experiment was performed on a Carri-Med CS 100 instrument equipped with a cup and vane geometry. Using this set-up the loss of water could easily be determined by weighing the sample before and after the experiment. When the sample was covered with a 5 mm layer of vacuum pump oil as described above 3% of water were lost after 16 days, resulting in an increase of the clay concentration from 2% w/w to 2.06% w/w. The corresponding increase in viscosity can be estimated by comparing $|\eta^*|$ data for different Laponite concentrations taken under similar conditions of shear and recovery history. The dependence of viscosity on clay concentration can be described by a power law relationship $|\eta^*| \sim c^a$, with $a = 2.5$. Thus, the viscosity increment due to the evaporation of water is about 10% and this effect is by far not sufficient to account for the increase of viscosity shown in Fig. 10. Note that the above value of the exponent a is in good agreement with values reported previously (14, 16).

The linear relationship between $\log |\eta^*|$ and $\log t$ shown in Figs. 6 through 10 corresponds to a power law

$$|\eta^*| \sim t^n \quad [3]$$

characterizing the kinetics of the thixotropic recovery of Laponite RD dispersions. A single exponent is valid throughout the time regime from 10 s up to 10^6 s.

From Fig. 5 an upper limit of 0.2 Pa·s for the initial value of $|\eta^*|$ ($t = 0$) is deduced for a clay concentration of 1% w/w. Since this value is much lower than the viscosity values obtained in the power law regime, the exponent n can be determined directly from the slopes of the straight lines fitted to the experimental data in Figs. 6–10 and a value of

$$n = 0.13 \pm 0.02 \quad [4]$$

is obtained independent of clay concentration and mechanical pretreatment.

SUMMARY AND CONCLUSION

The rheological properties of aqueous dispersions of the synthetic hectorite clay Laponite RD forming gel-like structures have been investigated. Special emphasis has been laid on the phenomenon of thixotropy. The structural recovery at rest after steady shear is considered a fundamental thixotropic process and has been characterized by small amplitude oscillatory shear measurements.

A monotonic increase of $|\eta^*|$ with time has been ob-

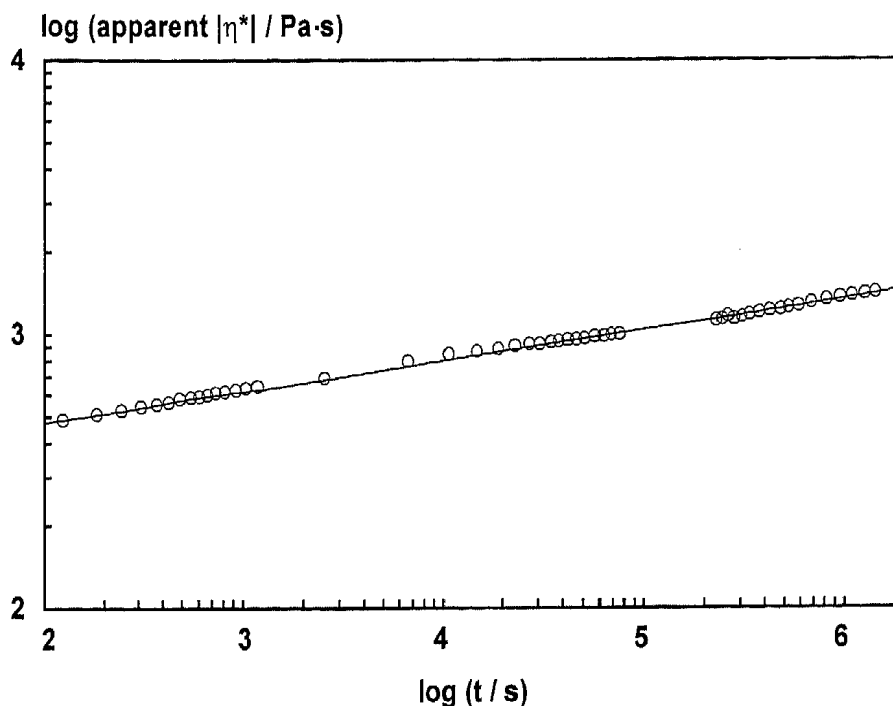


FIG. 10. Long term experiment (16 days) determining the recovery of $|\eta^*|$ after cessation of steady shear ($t = 30$ s; $\dot{\gamma} = 1000$ s $^{-1}$) for a 2% w/w dispersion of Laponite RD in 0.009 mol/dm 3 NaCl-solution, where oscillation $\omega = 6.28$ s $^{-1}$, $\dot{\gamma} < 0.01$. Performed on a Carri-Med CS 100 instrument with a cup and vane geometry.

served, and even in a long-term experiment lasting for 16 days no equilibrium viscosity value was reached, indicating that structural re-arrangements are still going on even after such a long time at rest.

A single power law $|\eta^*| \sim t^n$ holds within the time regime from 10 s to 10 6 s after cessation of steady shear. The exponent $n = 0.13 \pm 0.02$ is independent of clay concentration and mechanical pre-treatment of the material.

As far as the author knows this type of kinetics has not been reported for the thixotropic recovery of any clay dispersion before. First vague indications of the phenomenon have been given by relaxation measurements (14) where nonexponential stress decay is observed on a time scale of several hours and by SANS experiments (12) showing a strong anisotropic scattering pattern even 1 h after cessation of steady shear.

Moreover, our result does not fit the common definition of thixotropy, which implies that each shear rate is related to a unique equilibrium viscosity value and that this value is reached within a finite time (24).

Note that similar power law behavior with exponent $n = 0.18$ has been reported for the thixotropic recovery of flocculated suspensions of rod-like ferrite particles (25).

The experimental results reported here may be interpreted as follows:

The three-dimensional network structure of the clay dispersion is disintegrated into small flocs of particles or (less probably) into single platelets by application of shear forces. These flocs may exist as small domains of orientationally correlated particles (12, 14) or as aggregates flocculated in

a so-called house of cards like structure (1, 11). After cessation of steady shear a microscopic structural rearrangement of clay flocs and platelets takes place, setting up and reinforcing a network structure (showing up in the monotonic increase of $|\eta^*|$). According to the observed power law behavior with $n < 1$ the rate of change $d|\eta^*|/dt$ is monotonically decreasing with time, indicating a slowing down of the structural changes with increasing rigidity of the network. Therefore, the thixotropic reorganisation of the clay network can be interpreted as a cooperative, self-delaying process and the probability for an "imperfect" network link to move/jump into a position of lower free energy decreases with decreasing number of such "imperfections". Finally, the equilibrium state (minimum of free energy) of the whole network is reached only after infinite time and is characterised by an infinite viscosity or modulus G' ($\gg G''$), respectively.

A more detailed description of this process is not possible on the basis of our data. Moreover, it seems not to be appropriate, since the microscopic structure of the clay platelet network, especially the physical nature and structure of the so-called flocs, is still under discussion.

Similar self-delaying processes are observed for example in the aging of amorphous polymers (26) and in the precipitation from supersaturated solid solutions (27).

In the case of glassy polymers the segmental mobility M depends on the amount of free volume v_f , while on the other hand M determines the rate dv_f/dt at which v_f changes and, therefore, the state of zero mobility is not reached in a finite time.

In a supersaturated solid solution grains of a new phase grow by coalescence, i.e., the large grains grow by the incorporation of small ones, when an appreciable size is reached and the degree of supersaturation is only slight. The critical size $\langle x \rangle$ of stable domains increases with time as $t^{1/3}$. This result has been derived using rather general assumptions. To check whether it is relevant to the description of the thixotropic recovery of Laponite dispersions one either would have to derive a correlation between the domain size $\langle x \rangle$ and $|\eta^*|$ or would have to probe the microstructure/floc size of the clay dispersion directly by an appropriate scattering experiment. But both are beyond the scope of this paper.

ACKNOWLEDGMENTS

The author is indebted to J. Steidel and P. Sternal for the careful performance of the experimental work. Many helpful discussions with J. Rieger, H. M. Laun (Polymer Research Division, BASF AG), and N. J. Wagner (University of Delaware) are gratefully acknowledged. The Laponite RD powder was kindly supplied by Deutsche Solvay GmbH (Rheinsberg, Germany).

REFERENCES

1. van Olphen, H., "An Introduction to Clay Colloid Chemistry," 2nd ed. Wiley, New York, 1977.
2. van Olphen, H., and Fripiat, J. J. (Eds.), in "Data Handbook for Clay Minerals and Other Non-Metallic Minerals." OECD and Clay Minerals Society, Pergamon, Oxford, 1979.
3. Rand, B., Penkneec, E., Goodwin, J. W., and Smith, R. W., *J. Chem. Soc. Faraday Trans.* **76**, 225 (1980).
4. Sohm, R., and Tadros, T., *J. Colloid Interface Sci.* **132**, 62 (1989).
5. Neumann, B. S., *Rheol. Acta* **4**, 250 (1965).
6. Thompson, D. W., and Butterworth, J. T., *J. Colloid Interface Sci.* **151**, 236 (1990).
7. Avery, R. G., and Ramsey, J. D. F., *J. Colloid Interface Sci.* **109**, 448 (1986).
8. Rosta, L., and von Gunten, H. R., *J. Colloid Interface Sci.* **134**, 397 (1990).
9. Norrish, K., *Discuss. Faraday Soc.* **11**, 82 (1954).
10. Callaghan, I. C., and Ottewill, R. H., *Faraday Discuss. Chem. Soc.* **57**, 110 (1974).
11. van Olphen, H., *J. Colloid Sci.* **17**, 660 (1962).
12. Ramsey, J. D. F., and Lindner, P., *J. Chem. Soc. Faraday Trans.* **89**, 4207 (1993).
13. Morvan, M., Espinat, D., Lambard, J., and Zemb, Th., *Colloids Surf. A Physicochem Eng. Aspects* **82**, 193 (1994).
14. Mourchid, A., Delville, A., Lambard, J., Lecolier, E., and Levitz, P., *Langmuir* **11**, 1942 (1995).
15. Lockhart, N. C., *J. Colloid Interface Sci.* **74**, 509 (1980).
16. Ramsay, J. D. F., *J. Colloid Interface Sci.* **109**, 441 (1986).
17. Perkins, R., Brace, R., and Matijevic, E., *J. Colloid Interface Sci.* **48**, 417 (1974).
18. Fripiat, J., Cases, J., Francois, M., and Letellier, M., *J. Colloid Interface Sci.* **89**, 378 (1982).
19. Neumann, B. S., Samson, K. G., *Clay Miner.* **9**, 231 (1971).
20. Fitch, F. R., Jenness, P. K., Rangus, S. E., in "Advances in Measurement and Control of Colloidal Processes" (de Jaeger and Williams, Eds.), p. 292. Butterworth, Stoneham, MA, 1991.
21. Mewis, J., and de Bleyser, R., *J. Colloid Interface Sci.* **40**, 360 (1972).
22. Khandal, R. K., and Tadros, T., *J. Colloid Interface Sci.* **125**, 122 (1988).
23. Dzuy, N. Q., and Boger, D. V., *J. Rheol.* **29**, 335 (1985).
24. Berker, A., and van Arsdale, W. E., *Rheol. Acta* **31**, 119 (1992).
25. Kanai, H., and Amari, T., *Reports Prog. Polym. Phys. Jpn.* **34**, 71 (1991).
26. Struik, L. C. E., "Physical Aging in Amorphous Polymers and Other Materials." Elsevier, Amsterdam, 1978.
27. Lifshitz, I. M., and Slyozov, V. V., *J. Phys. Chem. Solids* **19**, 35 (1961).